Acta Neuropathol (2012) 123:853–860
DOI 10.1007/s00401-012-0993-5

ORIGINAL PAPER

CIC and *FUBP1* mutations in oligodendrogliomas, oligoastrocytomas and astrocytomas

Felix Sahm · Christian Koelsche · Jochen Meyer · Stefan Pusch · Kerstin Lindenberg · Wolf Mueller · Christel Herold-Mende · Andreas von Deimling · Christian Hartmann

Received: 21 February 2012 / Revised: 2 May 2012 / Accepted: 2 May 2012 / Published online: 17 May 2012

Abstract *CIC* and *FUBP1* mutations have recently been detected in oligodendrogliomas but not in oligoastrocytomas. However, allelic losses in the regions on chromosomal arms 19q and 1p harboring *CIC* and *FUBP1* are a common feature of both, oligodendrogliomas and oligoastrocytomas. To resolve this discrepancy, we analyzed *CIC* and *FUBP1* mutations in a set of primary brain tumors including 18 oligodendrogliomas and 42 oligoastrocytomas. In addition, we analyzed 10 astrocytomas and 16 glioblastomas with allelic losses on 19q as well as a set of 12 medulloblastomas for *CIC* mutations. *CIC* mutations were found in 15/18 oligodendrogliomas, 14/42 oligoastrocytomas and 3/10 preselected astrocytomas. With the exception of a single case, all *CIC* mutations occurred in tumors with combined 1p/19q losses. In contrast to oligodendrogliomas where *CIC* mutations were always detected along with 1p/19q co-deletion, *CIC* mutations were only found in 52 % of the 1p/19q co-deleted oligoastrocytomas. *FUBP1* mutations were detected in 7/61 tumors, all presenting with *CIC* mutations. *FUBP1* mutations appear to cluster in the DNA binding domain spanning exons 5–14. *CIC* and *FUBP1* mutations exclusively occurred in presence of either *IDH1* or *IDH2* mutations. Our data confirm *CIC* and *FUBP1* mutations in oligodendrogliomas and demonstrate the presence of these mutations in oligoastrocytomas.

Keywords CIC · FUBP1 · Oligodendroglioma · Oligoastrocytoma · 1p · 19q

Electronic supplementary material The online version of this article (doi:10.1007/s00401-012-0993-5) contains supplementary material, which is available to authorized users.

F. Sahm · C. Koelsche · W. Mueller · A. von Deimling (✉) · C. Hartmann
Department of Neuropathology, Ruprecht-Karls-Universität Heidelberg, Im Neuenheimer Feld 220/221, 69120 Heidelberg, Germany
e-mail: andreas.vondeimling@med.uni-heidelberg.de

F. Sahm · J. Meyer · S. Pusch · K. Lindenberg · A. von Deimling · C. Hartmann
Clinical Cooperation Unit Neuropathology G380, German Cancer Research Center (DKFZ), 69120 Heidelberg, Germany

C. Herold-Mende
Division of Neurosurgical Research, Department of Neurosurgery, Ruprecht-Karls-Universität Heidelberg, 69120 Heidelberg, Germany

Present Address:
C. Hartmann
Department for Neuropathology, Institute for Pathology, Hannover Medical School, Carl-Neuberg-Str. 1, 30625 Hannover, Germany

Introduction

Oligodendroglial tumors including oligodendrogliomas and oligoastrocytomas commonly exhibit joint allelic losses of chromosomal arms 1p and 19q. Just recently, strong candidates for the putative tumor suppressor genes in these regions have been proposed. Mutations in *CIC* mapping to chromosome 19q have been found in oligodendrogliomas [3, 14]. Likewise, mutations in *FUBP1* mapping to 1p have been detected in oligodendrogliomas, but only in one of these studies [3]. Oligoastrocytomas so far have not been examined thoroughly for *CIC* and *FUBP1* mutations and the sparse data currently available did not reveal alterations in these genes [14].

Human *CIC* is the homolog of the capicua gene in *Drosophila*. Capicua acts as downstream transcriptional repressor of receptor tyrosine kinase pathways mediating extracellular signals to gene regulation. Capicua regulation

is achieved by phosphorylation through MAP kinases [6]. The role of murine and human *CIC* has not been investigated in depth but it is involved in the development of granule cells. However, essential functional domains, such as DNA binding domains and critical phosphorylation sites, are conserved and functional. Thus, CIC is mainly expressed in undifferentiated tissue, pointing to a possible role in development [7]. *FUBP1* encodes a DNA binding protein shown to be involved in c-myc regulation [4].

Oligodendrogliomas with classical morphological features as well as diffuse astrocytomas are well-defined entities [9]. In contrast, oligoastrocytoma frequently poses diagnostic problems caused by the less stringent definition of sharing both, oligodendroglial and astrocytic morphology and by the problem of representative surgical sampling. This may result in considerable diagnostic variation among different observers. Therefore, the analysis of molecular genetic features of oligoastrocytomas has been hoped for solving classification problems. While combined 1p/19q losses are typical for oligodendrogliomas and *TP53* mutations are characteristic for diffuse astrocytomas, oligoastrocytomas unfortunately appear to exhibit both of these alterations [9]. *IDH* mutations are not helpful in distinguishing these entities due to a very high-mutation rate in all, diffuse astrocytomas, oligodendrogliomas and oligoastrocytomas [1]. Knowledge of the involvement of the recently detected *CIC* and *FUBP1* mutations may help to further clarify the classification of these tumors.

To resolve the current discrepancy regarding *CIC* mutations in oligodendrogliomas and oligoastrocytomas and to test the potential role of *CIC* in embryonal human tumors, we analyzed the entire coding sequence of *CIC* in a series of primary human brain tumors. We went on performing *FUBP1* analysis in all oligodendrogliomas, oligoastrocytomas and astrocytomas.

Materials and methods

Tumor specimens average patient age and sex ratio

We analyzed DNA extracted from fresh frozen material of 98 human brain tumors retrieved from the archive of the Department of Neuropathology, Institute of Pathology, Heidelberg. All tumors were diagnosed and classified according to the WHO classification of tumors of the nervous system [9]. The series consisted of 9 oligodendrogliomas WHO grade II (OII), 9 anaplastic oligodendrogliomas WHO grade III (OIII), 16 oligoastrocytomas WHO grade II (OAII), 26 anaplastic oligoastrocytomas (OAIII), 3 diffuse astrocytomas WHO grade II (AII), 7 anaplastic astrocytomas WHO grade III (AIII), 16 glioblastomas WHO grade IV (GBM), including 2 GBM of the giant cell variant as well as 12 medulloblastomas WHO grade IV (MBIV). Oligodendrogliomas were included as a verification set to compare the present study with previously published data. The series of diffuse astrocytomas and GBM was biased for the presence of allelic loss on 19q with some of the tumors also exhibiting additional loss of 1p.

Direct sequencing of *CIC FUBP1*, *IDH1* and *IDH2*

Fragments spanning all 20 exons of *CIC* were amplified using 20 ng each of the respective forward and reverse primer. Primer design was based on accession number NM_015125.3. Also, fragments spanning all 20 exons of *FUBP1* were amplified using 20 ng each of the respective forward and reverse primer. Primer design was based on accession number NM_003902.3. Primer sequences are given as supplemental data.

For PCR, 100 ng of DNA and HotStar 2× PCR Master Mix (Qiagen, Hilden, Germany) was employed. PCR was performed in a total volume of 30 µl, and included initial denaturation at 95 °C for 180 s, followed by 35 cycles with denaturation at 95 °C for 30 s, annealing at 56 °C for 25 s and extension at 72° C for 40 s. Two microliters of the amplification product were submitted to bidirectional sequencing using the BigDye Terminator v3.1 Sequencing Kit (Applied Biosystems, Foster City, CA, USA). Sequences were determined using a ABI 3500 Genetic Analyzer (Applied Biosystems) and the Sequence Pilot version 3.1 (JSI-Medisys, Kippenheim, Germany) software.

IDH1 exon 4 encompassing codon 132 and *IDH2* exon 4 encompassing codon 172 were subjected to analysis by direct sequencing using an ABI 3500 Genetic Analyzer as previously described [5].

Microsatellite analysis and multiplex ligation-dependent probe amplification (MLPA)

All samples were analyzed for loss of heterozygosity (LOH) of 1p and 19q employing at least three polymorphic microsatellite markers for each chromosomal arm as previously described [2].

MLPA was employed for detection of chromosomal losses on 1p and 19q in all oligodendrogliomas and oligoastrocytomas testing 15 loci on 1p and 8 loci on 19q. Analysis was performed using a commercially available kit (Salsa MLPA, P088, MRC Holland, Amsterdam, The Netherlands). The capability of MLPA to detect partial deletions has been demonstrated previously [13]. PCR products were separated and quantified on an ABI 3500 Genetic Analyzer (Applied Biosystems). Results were analyzed by the MLPA module in the Sequence Pilot 3.1 Software (JSI medical systems). Chromosomal regions were scored as under- or overrepresented if 2 or more

probes on 1p or 19q adjacent to each other exhibited a ratio smaller than 0.7 or above 1.3, respectively [13].

Immunofluorescence and immunohistochemistry

Sections from 2 archival cases with known 1p/19q-, *IDH*- and *CIC*-status were cut to 3 µm, deparaffinized and incubated in Ventana cell conditioner 1 (Ventana Medical Solutions, Tucson, USA) for 30 min followed by 5 % BSA blocking solution. Primary antibodies against CIC protein, recognizing an epitope spanning residues 1,150–1,200 (Abcam, Cambridge, UK; 1:50), and H09, binding mutant IDH1R132H protein (Dianova, Hamburg, Germany; 1:100) were applied for 2 h at room temperature. Secondary antibodies were anti-rabbit AlexaFluor 488 (Invitrogen, Carlsbad, USA; 1:500) and anti-mouse AlexaFluor 568, incubated for 30 min at room temperature. Slides were mounted with Vectashield Hardening Mounting medium, containing DAPI (Vector Labs, Burlingame, USA).

For immunohistochemistry, sections were processed on a Ventana BenchMark XT® immunostainer (Ventana Medical Systems, Tucson, AZ, USA). The Ventana staining procedure included pretreatment with cell conditioner 1 (pH 8) for 60 min, followed by incubation with anti-CIC (1:150) antibody at 37 °C for 32 min. Incubation was followed by Ventana standard signal amplification, UltraWash, counterstaining with one drop of hematoxylin for 4 min and one drop of bluing reagent for 4 min. For visualization, ultraView™Universal DAB Detection Kit was used.

Results

CIC mutations

For each tumor, data on the status of the *IDH* genes and on allelic losses on chromosomal arms 1p and 19q are compiled in Table 1.

CIC mutations were detected in 15/18 oligodendrogliomas encompassing 7/9 in OII and 8/9 OIII and in 14/42 oligoastrocytomas encompassing 6/16 in OAII and 8/26 OAIII. In diffuse astrocytomas preselected for 19q deletion, *CIC* mutations were detected in 3/10 diffuse astrocytomas encompassing 2/3 in AII and 1/7 in AIII. Of note, all *CIC* mutant astrocytomas presented with combined LOH 1p/19q. No *CIC* mutations were detected in the set of 16 glioblastomas and 12 medulloblastomas. The type of *CIC* mutations is given in Table 2.

The frequency of *CIC* mutations in oligodendrogliomas (83 %) was higher than in oligoastrocytomas (33 %) ($p < 0.002$; Fisher's Exact test). While in oligodendrogliomas all patients (100 %) with LOH 1p/19q carried a *CIC* mutation, only 13/25 (52 %) oligoastrocytoma patients with LOH 1p/19q carried a *CIC* mutation ($p < 0.002$; Fisher's Exact test). A single patient with OAII exhibited a *CIC* mutation but neither allelic losses on 1p nor 19q.

As previously described [3, 14], *CIC* mutations occurred throughout the coding sequence with an increased frequency in exon 5 and approximately similar numbers for missense and nonsense mutations.

FUBP1 mutations

DNA for *FUBP1* analysis was available from 61 tumors (Table 1). We detected *FUBP1* mutations in 7/61 tumors including 2 OII, 1 OIII, 2 OAII, 1 OAIII and in 1 AII. The type of *FUBP1* mutations is given in Table 2.

FUBP1 mutations appeared to cluster in the *FUBP1* DNA binding site spanning exons 5–14. In contrast to *CIC*, the predominant types of alterations in *FUBP1* were frameshift and nonsense mutations. Repetitive Poly-A sequences impaired the selection of optimal primers for exon 6 resulting in lack of data for nucleotide positions 397–412.

Allelic loss of 1p and 19q

Due to the limited number of markers analyzed by conventional microsatellite analysis, we could not safely conclude the extent of the deletions. Therefore, all oligodendrogliomas and oligoastrocytomas were also tested by MLPA. All oligodendrogliomas and oligoastrocytomas with losses exhibited deletion of the entire chromosomal arms.

Age and sex distribution

Mean age for the patient groups with *CIC* and *FUBP1* mutations was: OII 40 years, OIII 45 years, OAII 46 years, OAIII 42 years, AII 39 years, AIII 38 years (one patient). No significant differences were seen between patients with and without mutations, or within the groups of oligodendrogliomas (Student's t test $p > 0.24$), oligoastrocytomas (Student's t test $p > 0.4$), grade II tumors (Student's t test $p > 0.09$), grade III tumors (Student's t test $p > 0.14$), OII (Student's t test $p > 0.45$) and AII (Student's t test $p > 0.33$). Presence of only a single mutant or wild-type case in AIII and OIII, respectively, did not allow for statistical analysis. No significant differences in mutation rates were seen between male and female patients (Student's t test $p > 0.07$).

Immunofluorescence and immunohistochemistry

Two tumors with 1p/19q co-deletion and *IDH1*R132H mutation were analyzed. The OII (case 7) harbored a

Table 1 Diagnosis, *CIC*, *FUBP1*, 1p/19q and *IDH1/2* status

ID	Diagnosis	*IDH1/2*	1P	19q	*CIC*	*FUBP1*	ID	Diagnosis	*IDH1/2*	1P	19q	*CIC*	*FUBP1*
1	OII	R132H	LOH	LOH	**mut**	**mut**	51	OAIII	R132H	nd	nd	wt	wt
2	OII	R132H	LOH	LOH	**mut**	**mut**	52	OAIII	nd	LOH	LOH	wt	wt
3	OII	R132H	LOH	LOH	**mut**	wt	53	OAIII	R132H	LOH	LOH	wt	nd
4	OII	R132H	LOH	LOH	**mut**	wt	54	OAIII	R132H	ret	ret	wt	wt
5	OII	R132H	LOH	LOH	**mut**	nd	55	OAIII	R132H	ret	ret	wt	nd
6	OII	R132H	LOH	LOH	**mut**	wt	56	OAIII	R132H	LOH	LOH	wt	nd
7	OII	R132H	LOH	LOH	**mut**	wt	57	OAIII	wt	ret	ret	wt	wt
8	OII	R132H	ret	ret	wt	nd	58	OAIII	nd	LOH	LOH	wt	wt
9	OII	wt	ret	ret	wt	wt	59	OAIII	R132H	LOH	LOH	wt	wt
10	OIII	R132H	LOH	LOH	**mut**	wt	60	OAIII	R132H	LOH	LOH	wt	wt
11	OIII	R132H	LOH	LOH	**mut**	wt	61	AII	R132H	LOH	LOH	**mut**	wt
12	OIII	R132H	LOH	LOH	**mut**	wt	62	AII	R132H	LOH	LOH	**mut**	**mut**
13	OIII	R132H	LOH	LOH	**mut**	wt	63	AII	wt	ret	LOH	wt	nd
14	OIII	R132H	LOH	LOH	**mut**	wt	64	AIII	R132H	LOH	LOH	**mut**	wt
15	OIII	R132H	LOH	LOH	**mut**	wt	65	AIII	R132H	ni	LOH	wt	wt
16	OIII	R132H	LOH	LOH	**mut**	nd	66	AIII	R132H	LOH	LOH	wt	wt
17	OIII	R132H	LOH	LOH	**mut**	**mut**	67	AIII	R132H	ni	LOH	wt	wt
18	OIII	R132H	ret	ret	wt	wt	68	AIII	R132H	LOH	LOH	wt	wt
19	OAII	R132H	LOH	LOH	**mut**	wt	69	AIII	wt	ret	LOH	wt	wt
20	OAII	R132H	LOH	LOH	**mut**	nd	70	AIII	wt	ret	LOH	wt	wt
21	OAII	R132H	ret	ret	**mut**	wt	71	GBM	wt	LOH	LOH	wt	nd
22	OAII	R132H	LOH	LOH	**mut**	**mut**	72	GBM	wt	LOH	LOH	wt	nd
23	OAII	R132H	LOH	LOH	**mut**	wt	73	GBM	wt	ret	LOH	wt	nd
24	OAII	R132H	LOH	LOH	**mut**	**mut**	74	GBM	wt	LOH	LOH	wt	nd
25	OAII	R132H	ret	ret	wt	wt	75	GBM	wt	ret	LOH	wt	nd
26	OAII	R132H	LOH	LOH	wt	wt	76	GBM	wt	ret	LOH	wt	nd
27	OAII	wt	LOH	LOH	wt	wt	77	GBM	R132H	ret	LOH	wt	nd
28	OAII	R132H	ret	ret	wt	wt	78	GBM	wt	ret	LOH	wt	nd
29	OAII	R132H	ret	ret	wt	nd	79	GBM	wt	ret	LOH	wt	nd
30	OAII	R132H	LOH	LOH	wt	wt	80	GBM	wt	ret	LOH	wt	nd
31	OAII	R132H	LOH	LOH	wt	wt	81	GBM	wt	LOH	LOH	wt	nd
32	OAII	R132H	ret	ret	wt	wt	82	GBM	wt	LOH	LOH	wt	nd
33	OAII	R132H	ret	ret	wt	wt	83	GBM	wt	ret	LOH	wt	nd
34	OAII	R132H	ret	ret	wt	wt	84	GBM	wt	ret	LOH	wt	nd
35	OAIII	R132H	LOH	LOH	**mut**	wt	85	gcGBM	R132H	ret	LOH	wt	nd
36	OAIII	R172 K	LOH	LOH	**mut**	wt	86	gcGBM	wt	ret	LOH	wt	nd
37	OAIII	R132H	LOH	LOH	**mut**	**mut**	87	MBIV	nd	nd	nd	wt	nd
38	OAIII	R132H	LOH	LOH	**mut**	wt	88	MBIV	wt	nd	nd	wt	nd
39	OAIII	R132H	LOH	LOH	**mut**	wt	89	MBIV	wt	nd	nd	wt	nd
40	OAIII	R132H	LOH	LOH	**mut**	wt	90	MBIV	R132H	nd	nd	wt	nd
41	OAIII	R132H	LOH	LOH	**mut**	wt	91	MBIV	nd	nd	nd	wt	nd
42	OAIII	R132H	LOH	LOH	**mut**	wt	92	MBIV	nd	nd	nd	wt	nd
43	OAIII	R132H	ret	ret	wt	wt	93	MBIV	wt	ret	nd	wt	nd
44	OAIII	wt	ret	ret	wt	wt	94	MBIV	nd	nd	nd	wt	nd
45	OAIII	R132H	LOH	LOH	wt	wt	95	MBIV	wt	ret	ni	wt	nd
46	OAIII	R132H	ret	ret	wt	wt	96	MBIV	wt	ret	ni	wt	nd
47	OAIII	wt	ret	ret	wt	wt	97	MBIV	wt	ni	ret	wt	nd
48	OAIII	R132H	LOH	LOH	wt	wt	98	MBIV	wt	ret	ret	wt	nd

Table 1 continued

ID	Diagnosis	*IDH1/2*	1P	19q	*CIC*	*FUBP1*	ID	Diagnosis	*IDH1/2*	1P	19q	*CIC*	*FUBP1*
49	OAIII	R132C	ret	ret	wt	wt							
50	OAIII	R132H	ret	ret	wt	wt							

OII oligodendroglioma WHO grade II, *OIII* anaplastic oligodendroglioma WHO grade III, *OAII* oligoastrocytoma WHO grade II, *OAIII* anaplastic oligoastrocytoma WHO grade III, *AII* astrocytoma grade II, *AIII* anaplastic astrocytoma WHO grade III, *GBM* glioblastoma WHO grade IV, *gcGBM* giant cell glioblastoma WHO grade IV, *MBIV* medulloblastoma WHO grade IV, *R132H/C* amino acid substitution in mutant *IDH1*, *R172K* amino acid substitution in mutant *IDH2*, *LOH* loss of heterozygosity, *ret* both parental alleles retained, *wt* wild-type, *mut* mutant, *nd* not determined, *ni* not informative

missense and the OIII (case 10) a truncating nonsense mutation in *CIC* (Fig. 1). Immunofluorescent double labeling for mutant IDH1R132H and CIC protein yielded a signal for IDH1R132H protein in the tumor cells of both cases. CIC in tumor cells was only detected in the case with missense mutation. Subsequently, we performed immunohistochemistry on both tumors. Staining for CIC was observed in endothelial cells and all tumor cells of the OII with missense mutation (case 7), but only in very few tumor cells in the OIII with truncating mutation (case 10).

Discussion

CIC and *FUBP1* mutations in oligodendroglioma have recently been described. The present study investigated a validation set of oligodendrogliomas, a set of oligoastrocytomas, and a set of astrocytomas and glioblastomas biased for allelic losses on chromosomal arms 19q, as well as a set of medulloblastomas.

Validation set of oligodendrogliomas

Data from our validation set match with previous observations. *CIC* mutations were initially observed by deep sequencing in 18/34 (53 %) [3] and 20/29 (69 %) [14] oligodendrogliomas. By direct sequencing, we detected *CIC* mutations in 15/18 (83 %), thus confirming a high incidence in oligodendrogliomas and sensitivity of the methods applied. So far, *CIC* mutations have been tightly linked to the presence of combined allelic losses on 1p and 19q. This holds also true for our oligodendroglioma series with 15/18 (83 %) tumors exhibiting combined loss and 15/15 (100 %) of those tumors with combined loss also carrying a *CIC* mutation.

FUBP1 mutations were detected only in one of the two previous studies in 5/34 (15 %) [3] cases, while the other study did not find *FUBP1* mutations in 16 tumors [14]. We detected *FUBP1* mutations in 3/15 oligodendrogliomas with sufficient DNA available. We thus also confirm the incidence of *FUBP1* mutations in oligodendrogliomas comparable to that published previously [3].

Oligoastrocytomas

Oligoastrocytomas in our series exhibited *CIC* mutations in 14/42 (33 %) tumors. This contrasts previous findings not detecting *CIC* mutations in oligoastrocytomas. However, the previous study [14] analyzed by deep sequencing only 14 oligoastrocytomas without 1p/19q co-deletion, and all but one of our oligoastrocytomas with *CIC* mutation exhibited 1p/19q co-deletion. That study also examined an extension set containing 11 oligoastrocytomas, 3 of which harbored 1p/19q co-deletion, without detecting *CIC* mutations in exons 5 and 20 [14].

FUBP1 mutations have not previously been analyzed in these tumors and we detected *FUBP1* mutations in 3/13 (23 %) oligoastrocytomas with *CIC* mutation and 3/37 (8 %) of all oligoastrocytomas. We thus established the presence of *FUBP1* mutations in oligoastrocytomas.

The incidence of 1p/19q co-deletions in our oligoastrocytoma series was 25/42 (60 %) and thus lower than that in oligodendrogliomas with 15/18 (83 %). In both sets, *CIC* mutations with one exception were seen in 1p/19q co-deleted cases. Interestingly, the incidence of *CIC* mutations in oligodendrogliomas with 1p/19q co-deletion (15/15 cases; 100 %) was significantly higher ($p < 0.002$, Fisher's Exact test) than in oligoastrocytomas (13/25 cases; 52 %). Noteworthy, all oligodendrogliomas and oligoastrocytomas have been analyzed by MLPA and there was no difference in extent of deletion. This may point toward heterogeneity among 1p/19q co-deleted oligoastrocytomas and argues against reclassifying all oligoastrocytomas with 1p/19q co-deletions as oligodendrogliomas.

Astrocytomas, glioblastomas and medulloblastomas

In 10 astrocytomas selected for the presence of 19q deletions, we detected 3 *CIC* mutations among the 5 cases with a 1p/19q co-deletion. On the other hand, none of the 16 GBM including 5 cases with 1p and 19q deletion contained a *CIC* mutation. This most likely reflects the high-genomic instability of GBM with random occurrence of both, deletions on 1p and 19q. This interpretation finds support in the nearly invariant association of 1p/19q co-deletion with

Table 2 Characterization of *CIC* and *FUBP1* mutations

ID	Diagnosis	Exon	DNA sequence alteration	Codon change	Consequence
CIC					
1[a]	OII	20	c.4550-4552delAGA	KI1517-1518I	
2[a]	OII	5	c.601C>T	R201W	Missense
3	OII	5	c.601C>T	R201W	Missense
4	OII	1	Exon1 del 88bp		Frameshift
5	OII	13	c.3045insC	L1015 > 1150X	Frameshift
6	OII	4	c.453-2 a>t		Splice site mutation
7	OII	5	c.682C>T	R228W	Missense
10	OIII	6	c.877A>T	K293X	Nonsense
11	OIII	5	c.613A>C	N205H	Missense
12	OIII	17	c.4131-4156del26bp	Q1377 > 1431X	Frameshift
13	OIII	6	c.768-770delGAA	VK256-257V	
14	OIII	12	c.2904insCCCC	P968 > 1151X	Frameshift
15	OIII	10	c.1795delC	R599 > 727X	Frameshift
16	OIII	5	c.619T>A	F207I	Missense
17[a]	OIII	11	c.2719C>T	Q907X	Nonsense
19	OAII	5	c.643C>T	R215W	Missense
20	OAII	5	c.644G>A	R215Q	Missense
21	OAII	3	c.346G>T	V116L	Missense
22[a]	OAII	5	c.644G>T	R215Q	Missense
23	OAII	5	c.605G>A	R202Q	Missense
24[a]	OAII	5	c.716A>G	Y239C	Missense
35	OAIII	17	c.4135-4136delCT	L1379 > 1439X	Frameshift
36	OAIII	5	c.677A>G	D226G	Missense
37[a]	OAIII	10	c.2111-2112delCA	T704 > 709X	Frameshift
38	OAIII	14	c.3365-3366delTG	V1122 > 1149X	Frameshift
39	OAIII	3	c.278insGAGTGCTG	D93 > 207X	Frameshift
40	OAIII	10	c.1804-1814delAGACCCGAAAG	R602 > 685X	Frameshift
41	OAIII	5	c.633C>G	S211R	Missense
42	OAIII	5	c.682C>G	R228G	Missense
61	AII	7	c.1106-1109delAGAG	D369 > 375X	Frameshift
62[a]	AII	14	c.3348insC	P1116 > 1150X	Frameshift
64	AIII	5, 10	c.611T>C, c.1740insG	M204T, G580 > K689X	Missense, Frameshift
FUBP1					
1	OII	12	c.988C>T	R330X	Nonsense
2	OII	14	c.1244delC	P415 > 423X	Frameshift
17	OIII	13	c.1088insAG	G363 > 390X	Frameshift
22	OAII	10	c.816delA	G272 > 277X	Frameshift
24	OAII	6	c.262delCA	Q88 > 119X	Frameshift
37	OAIII	12	c.928-937delTTAAGCCAG	F310 > 318X	Frameshift
62	AII	10	c.806C>G	S269X	Nonsense

Numbering of bases showing alteration is given relative to the cDNA sequence. For deletions, the span of deleted bases is given, followed by the deletion size (del). For deletions of less than 10 bp, the deleted bases are also named. When the start position of the deletion is uncertain, the determinable ranges of bases deleted are shown. Insertion is indicated by ins followed by the bases inserted. Original amino acid and position of the residues in the protein is followed by the new amino acid for a missense mutation, X for a nonsense mutation, or by the position of the next in-frame stop codon for frameshift

[a] Mutations in both *CIC* and *FUBP1*

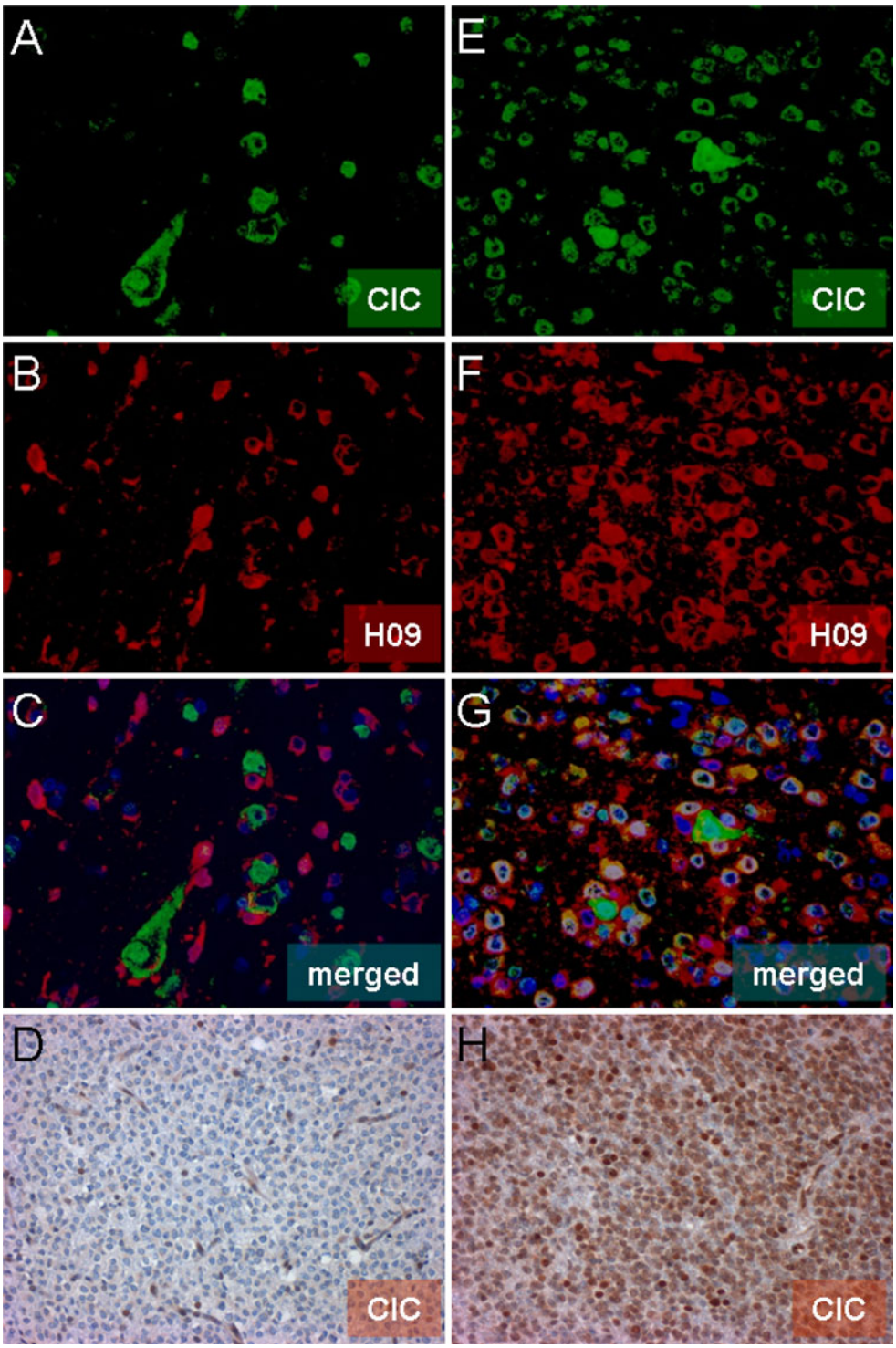

Fig. 1 Immunofluorescence for *CIC* (*green*) and mutant IDH1R132H protein (*red*) in the tumor infiltration area of two 1p/19q co-deleted, IDH1R132H mutant tumors. *CIC* nonsense mutation and 19q loss resulted in abrogation of CIC protein and mutually exclusive expression of tumor-specific mutated IDH1R132H (clone H09) and CIC protein. CIC expression is detectable in resident brain tissue (**a**–**d**). *CIC* missense mutation allows the detection of wild type and mutated CIC protein. CIC is seen in both, resident brain tissue and tumor cells characterized by expression of mutant IDH1R132H protein (**e**–**h**)

IDH mutations in the tumors with *CIC* mutations and in the absence of *IDH* mutations in all GBM samples harboring deletions on 1p and 19q (Table 1). The detection of *CIC* mutation and 1p/19 co-deletion in 3 diffuse astrocytomas may indicate mis-classification of these tumors and also may hint toward the limitations of routine assessment for

diagnosis. We point out that due to the preselected nature of the tumors included, our numbers for *CIC* mutations are not representative for all diffuse astrocytomas. A single *FUBP1* mutation was detected in 1 AII also carrying 1p/19q co-deletion and *IDH1* mutation.

The important role of *CIC* in granule cell development [7] and the report of a single *CIC* mutation in medulloblastomas [3] prompted us to screen 12 medullobastomas for the presence of *CIC* mutations. We did not detect mutations and this has also been shown by sequence analyses of all coding genes of medulloblastoma failing to detect *CIC* mutations [11]. In addition, high expression of CIC protein has been described in medulloblastomas further arguing against a prominent role of inactivating *CIC* mutations in these tumors [8].

Mutation types of *CIC* and *FUBP1*

Among 32 *CIC* mutations in our series, 16 presumably resulted in punctual protein alterations with 14 being of missense type and 2 representing in frame deletions of 1 amino acid each. The remaining 16 mutations were expected to result in severe alterations on the protein level with 12 constituting frameshift mutations, 2 nonsense mutations, 1 combined missense and frameshift mutation and 1 splice site mutation. The majority of mutations were located at the DNA-binding HMG-boxes, both in previous [3, 14] and our data sets.

All seven *FUBP1* mutations represented mutations causing severe protein alterations by producing frameshift mutations in five and nonsense mutations in two instances. The mutational spectrum for *CIC* [3, 14] and *FUBP1* [3] is comparable to that previously described. The majority of *FUBP1* mutations localized to the DNA binding domain spanning exons 5–14. The truncating nature of *FUBP1* mutations indicates a loss of function and contrasts the potential role of *FUBP1* in oligodendroglial tumors to that in liver cancer, where *FUBP1* overexpression is linked to tumor growth and migration [10, 12].

The loss of one parental gene copy in combination with the presence of considerable numbers of truncating mutations in both, *CIC* and *FUBP1* raises the possibility to detect complete protein loss with antibody-based detection systems. To this end, we applied double immunofluorescence with antibodies directed against the IDH1R132H mutated protein and against a C-terminal domain of CIC protein to two tumors, one with a truncation and one with a missense mutation. In the tumor with the truncating *CIC* mutation, mutually exclusive expression of CIC and IDH1R132H protein could be demonstrated while the tumor with missense mutations exhibited co-expression of CIC and IDH1R132H protein (Fig. 1).

In conclusion, we confirm the presence of *CIC* and *FUBP1* mutations in oligodendrogliomas, provide evidence for such mutations in oligoastrocytomas and a small fraction of astrocytomas and point out the heterogeneous mutation pattern within the group of 1p/19q co-deleted oligoastrocytomas.

Acknowledgments We wish to thank Antje Habel for skillful technical assistance and David Capper for critically reading the manuscript.

References

1. Balss J, Meyer J, Mueller W et al (2008) Analysis of the IDH1 codon 132 mutation in brain tumors. Acta Neuropathol 116:597–602
2. Bender B, Wiestler OD, von Deimling A (1994) A device for processing large acrylamide gels. Biotechniques 16:204–206
3. Bettegowda C, Agrawal N, Jiao Y et al (2011) Mutations in CIC and FUBP1 contribute to human oligodendroglioma. Science 333:1453–1455
4. Duncan R, Bazar L, Michelotti G et al (1994) A sequence-specific, single-strand binding protein activates the far upstream element of c-myc and defines a new DNA-binding motif. Genes Dev 8:465–480
5. Hartmann C, Meyer J, Balss J et al (2009) Type and frequency of IDH1 and IDH2 mutations are related to astrocytic and oligodendroglial differentiation and age: a study of 1010 diffuse gliomas. Acta Neuropathol 118:469–474
6. Kim Y, Andreu MJ, Lim B et al (2011) Gene regulation by MAPK substrate competition. Dev Cell 20:880–887
7. Lee CJ, Chan WI, Cheung M et al (2002) CIC, a member of a novel subfamily of the HMG-box superfamily, is transiently expressed in developing granule neurons. Brain Res Mol Brain Res 106:151–156
8. Lee CJ, Chan WI, Scotting PJ (2005) CIC, a gene involved in cerebellar development and ErbB signaling, is significantly expressed in medulloblastomas. J Neurooncol 73:101–108
9. Louis D, Ohgaki H, Wiestler O et al (2007) World Health Organization Classification of Tumours of the Central Nervous System. In: Bosman F, Jaffe E, Lakhani S et al (eds) World Health Organization Classification of Tumours, 4th edn. IARC, Lyon
10. Malz M, Weber A, Singer S et al (2009) Overexpression of far upstream element binding proteins: a mechanism regulating proliferation and migration in liver cancer cells. Hepatology 50:1130–1139
11. Parsons DW, Li M, Zhang X et al (2011) The genetic landscape of the childhood cancer medulloblastoma. Science 331:435–439
12. Rabenhorst U, Beinoraviciute-Kellner R, Brezniceanu ML et al (2009) Overexpression of the far upstream element binding protein 1 in hepatocellular carcinoma is required for tumor growth. Hepatology 50:1121–1129
13. Weller M, Berger H, Hartmann C et al (2007) Combined 1p/19q loss in oligodendroglial tumors: predictive or prognostic biomarker? Clin Cancer Res 13:6933–6937
14. Yip S, Butterfield YS, Morozova O et al (2012) Concurrent CIC mutations, IDH mutations, and 1p/19q loss distinguish oligodendrogliomas from other cancers. J Pathol 226:7–16